

Phase Coexistence in Driven One-Dimensional Transport

A. Parmeggiani,¹ T. Franosch,¹ and E. Frey^{1,2}

¹*Hahn-Meitner Institut, Abteilung Theorie, Glienicker Strasse 100, D-14109 Berlin, Germany*

²*Fachbereich Physik, Freie Universität Berlin, Arnimallee 14, D-14195 Berlin, Germany*

(Received 12 September 2002; published 28 February 2003)

We study a one-dimensional totally asymmetric exclusion process with random particle attachments and detachments in the bulk. The resulting dynamics leads to unexpected stationary regimes for large but finite systems. Such regimes are characterized by a phase coexistence of low and high density regions separated by domain walls. We use a mean-field approach to interpret the numerical results obtained by Monte Carlo simulations, and we predict the phase diagram of this nonconserved dynamics in the thermodynamic limit.

DOI: 10.1103/PhysRevLett.90.086601

PACS numbers: 72.70.+m, 02.50.Ey, 05.40.-a, 64.60.-i

Even some of the simplest driven diffusive systems in one dimension show surprisingly rich and complex behavior which is rather unexpected when looked at with experience gained from equilibrium phenomena [1]. Particularly illuminating examples are boundary-induced phase transitions in driven one-dimensional (1D) transport processes, such as the totally asymmetric simple exclusion process (TASEP). The model, originally proposed in [2], consists of particles hopping unidirectionally with hard-core exclusion along a 1D lattice. Because of conservation of the particle current in the bulk, the rates of incoming or outgoing particles at the boundaries drive the system to nontrivial stationary states [3]. The resulting phase diagram shows continuous and discontinuous transitions of the average density of particles in the limit of large system sizes. These results were obtained first in mean-field theory and then extended when a complete analytical solution was presented solving explicitly the recursion relations of the model or using a matrix product ansatz technique [4].

The TASEP is one of many examples for driven systems with stationary nonequilibrium states, which cannot be described in terms of Boltzmann weights. This has to be contrasted with processes like the bulk adsorption/desorption kinetics of particles on a lattice coupled to a reservoir [“Langmuir kinetics” (LK)], whose stationary state is well described within standard concepts of equilibrium statistical mechanics. Here particles adsorb at an empty site or desorb from an occupied one with fixed respective kinetic rates obeying detailed balance. The bulk density profile at equilibrium is described by a *Langmuir isotherm*, determined solely by the ratio of the two kinetic rates [5], as given by the Gibbs ensemble. Because of the presence of the particle reservoir there is no conservation of particles and no net particle current in the bulk. It is interesting to ask what can be expected in coupling two processes which have genuinely different dynamics and stationary states, like TASEP with open boundaries and LK.

In this Letter, we relax the constraint that the conserved dynamics in the bulk imposes to the TASEP by

allowing particle attachment and detachment. We are interested in the limit where the kinetic rates are such that the incoming and outgoing fluxes of particles at the boundaries and in the bulk are comparable. This implies that a particle, injected at the boundary or attached somewhere in the bulk, remains long enough on the lattice to move a finite fraction of the total system size. New phenomena are expected in the regime of competition between TASEP and LK for a large but finite system. Of course, the dynamics in an infinitely large system would be completely dominated by the bulk adsorption and desorption rates. It turns out that the presence of the kinetic rates significantly change the picture of TASEP, producing a completely reorganized phase diagram. We shall show by computer simulations and mean-field arguments that, in this nonconserved dynamics, one can have phase coexistence where low and high density phases are separated by stable discontinuities in the density profile.

The model we discuss here is directly inspired by the unidirectional motion of many motor proteins along cytoskeletal filaments [6]. Motors advance along the filament while attachment and detachment of motors between the cytoplasm and the filament occur [7]. Recently, it has been shown that such dynamics can be relevant for modeling the filopod growth in eukaryotic cells produced by motor proteins interacting within actin filaments [8].

We consider a 1D lattice composed of sites $i = 1, \dots, N$ (Fig. 1). The configurations are described in terms of occupation numbers $n_i = 1$ for a site occupied by a particle and $n_i = 0$ for an empty site (vacancy). The dynamics is determined by a master equation for the probabilities to find a particular configuration $\{n_i\}$. We

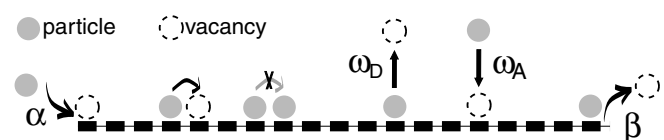


FIG. 1. TASEP scheme with bulk attachment/detachment.

apply the following dynamical rules. For each time step, a site i is chosen at random. A particle at site i can jump to site $i + 1$ if unoccupied (we fix units of time by putting this rate equal to unity). In the bulk $i = 2, \dots, N - 1$, a particle can also leave the lattice with a site-independent detachment rate ω_D or fill the site (if empty) with a rate ω_A by attachment. At the boundaries, a particle can fill a vacancy with a rate α at site $i = 1$, or a vacancy can be formed by removing a particle from the lattice with a rate β at site $i = N$. We refrain from giving explicitly the master equation for the probabilities. Correlations induced into the many-particle problem can be conveniently studied within an operator representation in Fock space [9]. Then the equations of the bulk dynamics read

$$\frac{dn_i}{dt} = n_{i-1}(1 - n_i) - n_i(1 - n_{i+1}) + \omega_A(1 - n_i) - \omega_D n_i, \quad (1a)$$

while at the boundaries one obtains

$$\begin{aligned} dn_1/dt &= \alpha(1 - n_1) - n_1(1 - n_2), \\ dn_N/dt &= n_{N-1}(1 - n_N) - \beta n_N. \end{aligned} \quad (1b)$$

By taking averages [10] one observes that in order to compute the time evolution of $\langle n_i(t) \rangle$ one needs the corresponding averages of higher order correlations. In order to obtain an exact solution, elaborate techniques are necessary. We restrict the discussion to Monte Carlo simulations (MCS) and a mean-field approximation (MFA) which we shall apply below.

The system exhibits a particle-hole symmetry in the following sense. A jump of a particle to the right corresponds to a vacancy move by one step to the left. Similarly, a particle entering the system at the left boundary can be interpreted as a vacancy leaving the lattice, and vice versa for the right boundary. Attachment and detachment of particles in the bulk is mapped to detachment and attachment of vacancies, respectively.

We are interested in large system sizes ($N \gg 1$) and, eventually, in the ‘‘thermodynamic limit’’ $N \rightarrow \infty$. In this case, the study of the competition between bulk and boundary dynamics requires that the kinetic rates decrease simultaneously with the system size. More precisely, we define the ‘‘reduced’’ rates Ω_A and Ω_D as $\Omega_A = \omega_A N$ and $\Omega_D = \omega_D N$, keeping $\Omega_A, \Omega_D, \alpha, \beta$ fixed as $N \rightarrow \infty$. Note that the binding constant $K = \omega_A/\omega_D$ remains unchanged when passing to the thermodynamic limit. Moreover, for $\omega_A = \omega_D = 0$, one arrives back at the TASEP respecting the same particle-hole symmetry described above.

We have performed extensive computer simulations [11] to obtain the average density profile in the stationary state. We illustrate typical phenomena by following a path in parameter space along curves with fixed α, β , and K while increasing $\Omega_D = \Omega_A/K$. Figure 2(a) shows the density profile for three different values of the kinetic rates. At small kinetic rates, $\Omega_A, \Omega_D \ll \alpha, \beta$, the average

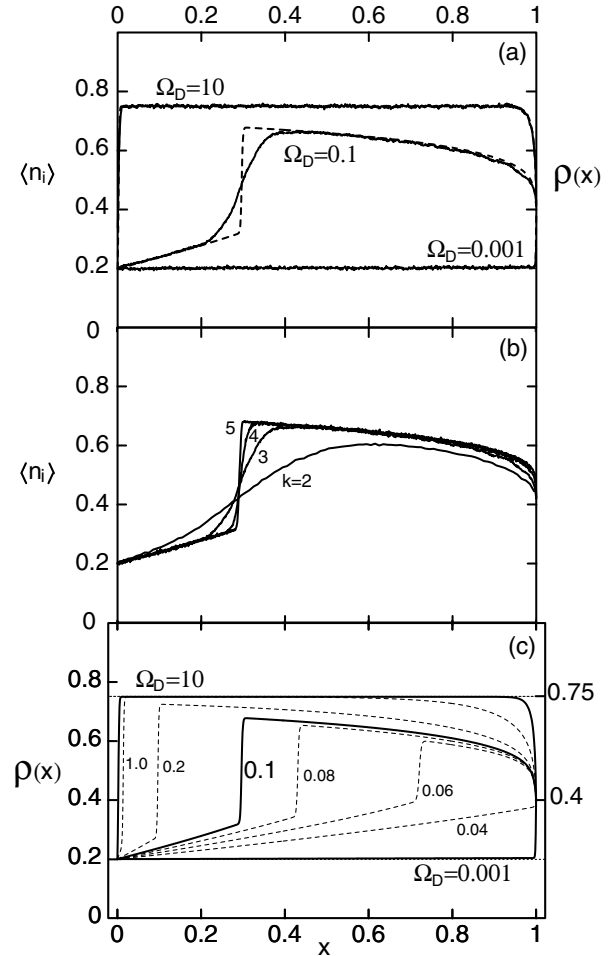


FIG. 2. (a) Average density profile $\langle n_i \rangle$ computed by MCS (continuous line) and average density profile $\rho(x)$ computed by numerical integration of MFA stationary state Eqs. (2) (dashed line) in the rescaled variable $x = i/N$ for $N = 10^3$ with $\alpha = 0.2$, $\beta = 0.6$, $K = 3$, and different kinetics rates Ω_D indicated in the graph. (b) MCS average density profile for different system sizes, same α, β, K as before, and $\Omega_D = 0.1$. The width of the steep rise decreases with increasing system sizes $N = 10^k$ with $k = 2, 3, 4, 5$ indicated in the graph. (c) MFA average density profile for $\varepsilon = 10^{-3}$, same α, β, K as before, and different kinetic rates Ω_D indicated in the graph. The horizontal dashed line for $\rho(x) = 0.75$ represents the Langmuir isotherm for $K = 3$.

density $\langle n_i \rangle$ in the bulk is practically constant and close to the low-density value predicted by the TASEP, $\langle n_i \rangle = \alpha$. Conversely, at high kinetic rates the bulk profile is structureless and essentially determined by the well-known ratio $K/(1 + K)$ of Langmuir equilibrium density [12]. A new feature appears for intermediate rates, $\Omega_D = 0.1$, precisely when bulk and boundary dynamics compete. The density exhibits a nonmonotonic structure in bulk, characterized by a region of low and high density connected by a steep rise.

Figure 2(b) shows the density profile for different system sizes. One observes a decrease of the width of

the transition region as the number of sites is increased. The simulation suggests a discontinuity of the profile in terms of the rescaled variable $x = i/N$ upon approaching the infinite system limit. A preliminary finite size scaling analysis is compatible with a rescaled transition width which scales as $N^{-\nu}$ with $\nu \approx 0.5$. This is very different from the mean-field result, $\nu_{\text{MFA}} = 1$ [13]. Thus we have identified an intermediate parameter range where low and high density phases coexist separated by a sharp domain wall (DW). We also find that the discontinuity in the density seems to be stable or at least localized in a small region compared to the system size [15]. This has to be contrasted with the domain wall (“shock”) found in the TASEP right at the phase boundary between the high- and low-density phases ($\alpha = \beta < 1/2$) which is delocalized and moves as a random walker once it is far from the system boundaries [9].

Phenomena like phase separation/coexistence have previously been observed in nonhomogeneous systems with open boundaries like TASEP with isolated localized defects [16,17]. The location of the domain walls are expected and found to be identical to the defect positions. In contrast, the location of the DW in our homogenous model is self-tuned and determined by the values of the kinetic rates (see below). In systems with periodic boundary conditions (which are not the subject of this Letter) phase separation has been found in TASEP with a blockage [18], quenched disorder [19], or in homogeneous systems with multispecies particle dynamics [20,21] (see for a general criterion [22]).

To rationalize all these findings we have developed a mean-field theory. Defining $\rho_i = \langle n_i \rangle$, the MFA consists of taking the average of Eqs. (1a) and (1b) and factorizing the two-site correlations, $\langle n_i n_{i+1} \rangle = \rho_i \rho_{i+1}$. Then Eqs. (1a) and (1b) display the same form provided that the binary occupation number n_i is replaced by the continuous variable ρ_i with $0 \leq \rho_i \leq 1$. The equations are now interpreted as ordinary differential equations.

To obtain an analytically tractable system of equations we have coarse-grained the discrete lattice with lattice constant $\varepsilon = L/N$ to a continuum. For fixed total length $L = 1$ and $N \rightarrow \infty$, $\varepsilon \rightarrow 0$ one gets the nonlinear differential equation for the average profile in the stationary state,

$$\frac{\varepsilon}{2} \partial_x^2 \rho + (2\rho - 1) \partial_x \rho + \Omega_A (1 - \rho) - \Omega_D \rho = 0, \quad (2)$$

where positions are measured by the rescaled variable $x = i/N$, $0 \leq x \leq 1$. Equations (1b) translate now to boundary conditions for the density field, $\rho(0) = \alpha$ and $\rho(1) = 1 - \beta$. One observes that MFA respects the particle-hole symmetry mentioned above, provided that when $\rho(x) \mapsto 1 - \rho(1 - x)$ one interchanges $\alpha \leftrightarrow \beta$, $\Omega_A \leftrightarrow \Omega_D$. Because of this property we can restrict the discussion to the case $\Omega_A > \Omega_D$ [23]. The numerical mean-field solutions are included in Fig. 2(a) for different values of Ω_D . We find good agreement of MFA compared

with MCS for the full range of kinetic rates in the limit of large N .

In analogy with fluid dynamics, to describe these results one considers an effective current density which for our problem reads $j = -(\varepsilon/2) \partial_x \rho + \rho(1 - \rho)$. Abbreviating the fluxes from and to the reservoir by $\mathcal{F}_A = \Omega_A (1 - \rho)$ and $\mathcal{F}_D = \Omega_D \rho$, Eq. (2) can be read as a balance equation: $\partial_x j = \mathcal{F}_A - \mathcal{F}_D$. Since there are two boundary conditions one has to be careful when discarding the second derivative in (2) for a small prefactor ε . The average profile is then governed by similar physics as the Burgers’s equation in the inviscid limit [16]. Generically one expects shocks (here DW) in the bulk and density layers at the boundaries (“boundary layers”). Crossing a DW, the current j remains continuous in the limit $\varepsilon \rightarrow 0$, while boundary layers form whenever the density associated with the bulk current does not fit the boundary condition. To better understand these features, we have explored the dependence of the density profile $\rho(x)$ on Ω_D for fixed α , β , and K [see Fig. 2(c)]. For small kinetic rates, $\Omega_D = 10^{-3}$, the profile is close to the one expected from TASEP, with a boundary layer bridging the bulk density up to $\rho = 1 - \beta$ [not resolved in Fig. 2(c)]. Increasing Ω_D the slope of the bulk density increases. For $\Omega_D > 0.05$, MFA connects a region of low density (LD), i.e., $\rho(x) < 1/2$, to a high density (HD) region, $\rho(x) > 1/2$, by a DW. Whereas the solution close to the left boundary is smooth, one finds a boundary layer at the right end bridging densities $\rho = 1/2$ down to $\rho = 1 - \beta$. For larger Ω_D the DW moves to the left, while the slope of the LD region increases and the HD profile flattens approaching the Langmuir density value $K/(K + 1)$. For $\Omega_D > 1$ the DW remains practically localized at the left boundary. Note that the DW location strongly depends on typical values of the bulk kinetic rates when they are comparable with the boundary rates α and β .

In the inviscid limit $\varepsilon \rightarrow 0$ the complete phase diagram can be obtained analytically within MFA, up to some treatment of the density discontinuities. Interestingly, the solution found is never given by either constant low/high density profiles as in TASEP or the Langmuir isotherm, but by a completely new set of solutions [14].

The mean-field analytical solution allows one to draw the phase diagram and compare it to TASEP. Figure 3 represents a cut through the phase diagram for $\Omega_D = 0.1$ and $K = 3$ with α and β used as control parameters. One finds an extended LD-HD coexistence region separating a LD and a HD phase. At the boundaries of the coexistence region, the DW between the low and high density phases are located in the proximity of the open ends of the 1D lattice. For small α the DW develops at the right end, $x = 1$, and moves to the left as α increases. At the phase boundary between the coexistence region and the HD phase, the DW is located at the left end of the lattice, $x = 0$. In both cases, when the DW enters and leaves the lattice, it matches with a boundary layer con-

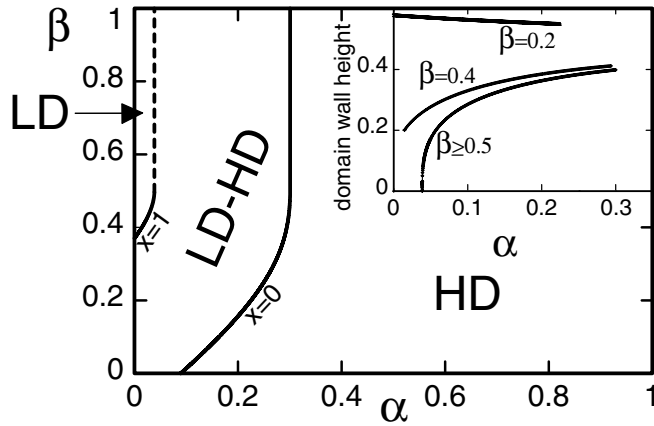


FIG. 3. Phase diagrams obtained by the exact solution of the stationary mean-field Eq. (2) in the inviscid limit for $K = 3$ and $\Omega_D = 0.1$. The inset shows the dependence of the DW amplitude on α for different values of β .

necting the bulk density with the density given by the corresponding boundary condition. (In this case, boundary layers appear only for $\alpha > 1/2$ and/or $\beta > 1/2$.) MFA shows that the bulk density profile becomes independent of β for $\beta > 1/2$. Hence, in this regime for a given α only the magnitude of the boundary layers changes, but not the profile of the bulk density. This explains the vertical phase boundaries of the coexistence region for $\beta \geq 1/2$.

In addition to its location the DW is also characterized by its height (see Fig. 3). For $\beta < 1/2$ we find that the height discontinuously jumps to a finite value upon entering the coexistence region from the LD phase. This has to be contrasted with the case $\beta \geq 1/2$ where the phase transition from the LD to the coexistence phase is characterized by a continuous increase in the height of the DW (compare the dashed line in Fig. 3). In MFA we find that both DW amplitude and position exhibit power law behavior with $(\alpha - \alpha_c)^{1/3}$ and $(\alpha - \alpha_c)^{2/3}$, respectively. At the phase boundary to the HD phase the DW height always jumps to zero discontinuously.

Working out the complete rich scenario for different Ω_A and Ω_D in the limit $N \gg 1$ needs a detailed analysis of the phase diagram [14]. We just mention that the original maximal current phase of the TASEP appears for $\Omega_A = \Omega_D$ only, where the Langmuir density is valued to $1/2$. This can be proved numerically as well as analytically. Conversely, as soon as $\Omega_A \neq \Omega_D$, MFA predicts that such a phase continuously disappears in favor of a HD phase if $\Omega_A > \Omega_D$ (respectively, an LD phase if $\Omega_A < \Omega_D$).

The authors thank P. Benetatos and J.E. Santos for useful discussions and comments. This work was partially funded by the DFG under Contracts No. FR 850/4 and No. SFB 413. A.P. is supported by a European Community Marie-Curie Fellowship, Contract No. HPMF-CT-2002-01529.

- [1] B. Schmittmann and R.K.P. Zia, in *Phase Transitions and Critical Phenomena*, edited by C. Domb and J.L. Lebowitz (Academic Press, London, 1995), Vol. 17.
- [2] J.T. MacDonald, J.H. Gibbs, and A.C. Pipkin, *Biopolymers* **6**, 1 (1968).
- [3] J. Krug, *Phys. Rev. Lett.* **67**, 1882 (1991).
- [4] B. Derrida, E. Domany, and D. Mukamel, *J. Stat. Phys.* **69**, 667 (1992); G. Schütz and E. Domany, *J. Stat. Phys.* **72**, 277 (1993); B. Derrida *et al.*, *J. Phys. A* **26**, 1493 (1993).
- [5] R.H. Fowler, *Statistical Mechanics* (Cambridge University Press, Cambridge, 1936).
- [6] A. Alberts *et al.*, *The Molecular Biology of the Cell* (Garland, New York, 1994).
- [7] Our model could also be relevant for studies of surface adsorption and growth in the presence of biased diffusion or of traffic models with bulk on-off ramps. See, e.g., *Nonequilibrium Statistical Mechanics in One Dimension*, edited by V. Privman (Cambridge University Press, Cambridge, 1997) and D. Chowdury *et al.*, *Phys. Rep.* **329**, 199 (2000).
- [8] K. Kruse and K. Sekimoto, *Phys. Rev. E* **66**, 031904 (2002).
- [9] For a review see, e.g., G.M. Schütz, in *Phase Transitions and Critical Phenomena*, edited by C. Domb and J.L. Lebowitz (Academic Press, San Diego, 2001), Vol. 19.
- [10] The notion of averaging is nontrivial since the system is far from equilibrium. Nevertheless, one expects the initial state to relax to a stationary ensemble over which averages should be taken.
- [11] MCS were performed with random sequential updating in discrete time: at each time step, a site is chosen at random and the dynamical rules are applied. Time and sample averages have been evaluated. The resulting profiles coincide in both averaging procedures for given parameters and different system sizes. In simulations for Figs. 2(a) and 2(b) stationary profiles have been obtained over 10^5 time averages (with a typical time interval of $\sim 10N$ between each average step).
- [12] In this case, during the detachment and attachment processes, we consider a constant particle concentration in the reservoir c_r (i.e., $c_r = 1$).
- [13] Upon introducing $x' = x/\varepsilon$, a scaling analysis of Eq. (2) shows that the domain wall width scales as $\nu_{\text{MFA}} = 1$ [14].
- [14] A. Parmeggiani, T. Franosch, and E. Frey (unpublished).
- [15] As a simple test, we artificially shifted the front of the discontinuity and let the system evolve in time. The discontinuity always moved back to its initial position.
- [16] S.A. Janowsky and J.L. Lebowitz, *Phys. Rev. A* **45**, 618 (1992).
- [17] A.B. Kolomeisky, *J. Phys. A* **31**, 1153 (1998).
- [18] G. Schütz, *J. Stat. Phys.* **71**, 471 (1993).
- [19] G. Tripathy and M. Barma, *Phys. Rev. E* **58**, 1911 (1998).
- [20] R. Lahiri and S. Ramaswamy, *Phys. Rev. Lett.* **79**, 1150 (1997); R. Lahiri, M. Barma, and S. Ramaswamy, *Phys. Rev. E* **61**, 1648 (2000).
- [21] M.R. Evans *et al.*, *Phys. Rev. E* **58**, 2764 (1998).
- [22] Y. Kafri *et al.*, *Phys. Rev. Lett.* **89**, 035702 (2002).
- [23] The case $\Omega_A = \Omega_D$ introduces new symmetries [14].